2. V. N. Chelomei, "Paradoxes in mechanics caused by vibrations," Dokl. Akad. Nauk SSSR, 270, No. 1 (1983).
3. B. A. Lugovtsov and V. L. Sennitskii, "Motion of a body in a vibrating fluid," ibid., 289, No. 2 (1986).
4. A. Rosato, K. J. Strandburg, F. Prinz, and R. H. Swedsen, "Why the Brazil nuts are on top: size segregation of particulate matter by shaking," Phys. Rev. Lett., 58, No. 10, (1987).
5. N. A. Logachev (ed.), Geology and Seismology of Regions of the Baikal-Amur Trunk Line [in Russian], Nauka, Novosibirsk (1983).

MOTION OF A CHAIN OF BUBBLES IN A VERTICAL CHANNEL WITH A VISCOUS FLUID

P. K. Volkov

UDC 532.529.6

Regular chains of nearly identically shaped bubbles moving one after the other are seen in bubble towers and in the uniform passage of gas bubbles through a tube. The upward velocity of the bubbles in these cases will obviously differ from the velocity of a single bubble of the same size, while the pattern of flow will depend to a significant extent on the distance between the bubbles. There are still serious obstacles to conducting theoretical and experimental studies of such bubble motion. The study [1] – where Nakorjakov et al. obtained the longitudinal components of the velocity vector across a tube behind a bubble and measured the friction on the tube wall – might be the only investigation to give some quantitative picture of the hydrodynamics of the process.

In the present study, we propose an algorithm for numerically solving the problem of the steady motion of a chain of bubbles in a viscous fluid within a vertical tube under the influence of buoyancy. Results are obtained for the case when the tube wall has almost no effect on the rise of the bubbles and the case when this effect is decisive.

1. Formulation of the Problem. In the coordinate system connected with the center of mass of the chain of bubbles, the tube moves downward at a constant velocity u equal to the upward velocity of each bubble and the fluid flows past the chain. In this case, the motion of the entire chain can be described by examining the flow past a single bubble. Since the problem is periodic, the flow pattern will be the same over the distances L up and down from the center of mass of the bubble; the period will be equal to 2L.

We introduce a spherical coordinate system (r, θ, φ) whose origin O coincides with the center of mass of the bubble (Fig. 1). Let $r = R(\theta)$ $(\theta \in [0, \pi])$ be the equation of the surface of the bubble and R_k be the radius of the tube. With allowance for the axial symmetry of the problem, the Navier–Stokes equations of a viscous incompressible fluid in the variables ω (curl) and ψ (stream function) have the same form as in [2, 3].

The boundary conditions differ from those described in [3] only in the sections Γ_1 $(r = L/\cos\theta,\ \theta \in [0, \theta^*])$ and Γ_2 $(r = -L/\cos\theta,\ \theta \in [\pi - \theta^*, \pi]$, $\tan\theta^* = R_k/L)$, where we assign periodicity conditions reflecting the fact that the values of the velocity functions and their derivatives over normals to the boundaries Γ_1 and Γ_2 coincide. It follows from [4] that, in terms of the curl ω and stream function ψ, they have the following form (where the z axis is directed along the tube)

$$\psi|_{\Gamma_1} = \psi|_{\Gamma_2}, \quad \partial\psi/\partial z|_{\Gamma_1} = \partial\psi/\partial z|_{\Gamma_2},$$
$$\omega|_{\Gamma_1} = \omega|_{\Gamma_2}, \quad \partial\omega/\partial z|_{\Gamma_1} = \partial\omega/\partial z|_{\Gamma_2}. \tag{1.1}$$

Novosibirsk. Translated from Zhurnal Prikladnoi Mekhaniki i Tekhnicheskoi Fiziki, No. 3, pp. 87-91, May-June, 1991. Original article submitted October 25, 1988.

0021-8944/91/3203-0379$12.50

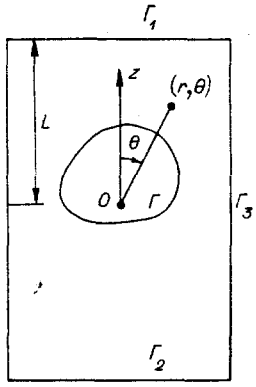

Fig. 1

With conditions (1.1), the problem obviously differs from that which was solved in [3] – where the velocity vector was given at the inlet and outlet. Conditions (1.1) mean that the profile of the velocity vector at the boundaries Γ_1, Γ_2 must be found simultaneously with the flow functions.

2. Algorithm for Solving the Problem. Since the only factor complicating the problem is the boundary conditions, we will solve it by the method described in [3]. Making the substitution of variables $\eta = (r - G(\theta))/(R(\theta) - G(\theta))$, $\theta' = \theta$ changes the flow region to a rectangle $[0, 1] \times [0, \pi]$. Here, the function $r = G(\theta)$ ($\theta \in [0, \pi]$) gives the equation of the boundary, which consists of three parts: Γ_1, Γ_2, Γ_3. At $\eta = 0$, Eqs. (1.1) take the form

$$\begin{aligned} &\psi|_{\Gamma_1} = \psi|_{\Gamma_2}, \quad (A\psi_\eta + B\psi_\theta)|_{\Gamma_1} = (A\psi_\eta + B\psi_\theta)|_{\Gamma_2}, \\ &\omega|_{\Gamma_1} = \omega|_{\Gamma_2}, \quad (A\omega_\eta + B\omega_\theta)|_{\Gamma_1} = (A\omega_\eta + B\omega_\theta)|_{\Gamma_2}, \end{aligned} \tag{2.1}$$

where $A = (\cos\theta + (G'/G)\sin\theta)/(R - G)$; $B = -\sin\theta/G$.

We used the difference scheme and the algorithm described in [5] to numerically solve the problem. However, two factors kept us from making direct use of the scheme in [5].

First of all, on Γ_3 there are two conditions for the function ψ and no conditions for ω. This situation is typical of problems solved in the variables of stream function ψ and curl ω and containing conditions of adhesion to solid walls. Proceeding similarly to [6], we obtain a condition for ω on Γ_3 with the use of the equations of motion:

$$\begin{aligned} \omega = \frac{G^2 + G'^2}{2(R-G)^2 G^3 \sin\theta}\Bigg[&\frac{2}{h_1^2}(\psi_1 - \psi_2 + h_1\psi_\eta) + \frac{2G'(R-G)}{G^2 + G'^2}\psi_{\eta\theta} + \\ &+ \frac{(R-G)\left(G'' - \dfrac{\cos\theta}{\sin\theta}G\right) - 2G'(R' - G')}{G^2 + G'^2}\psi_\eta\Bigg]. \end{aligned} \tag{2.2}$$

Here, h_1 is the mesh of the difference grid with respect to η; ψ_1 is the value of ψ on the wall Γ_3; ψ_2 is the value of ψ at the distance h_1 from the wall; ψ_η, $\psi_{\eta\theta}$ are calculated in accordance with Eq. (1.6) from [3]. To obtain a stable computation with condition (2.2), it is necessary to perform the following relaxation procedure [7]: $\omega^{k+1} = \alpha\omega + (1 - \alpha)\omega^k$ [where k is the number of the iteration; α is chosen experimentally ($\sim h_1$)].

Secondly, conditions (2.1) connect the functions and their derivatives on different sections of the boundary $\eta = 0$. We obtain formulas to calculate ψ and ω on Γ_1 and Γ_2, having exactly satisfied (2.1) in the process. As in [5], we will use the method of a stabilizing correction to solve the problem of determining ψ and ω. Obvious difficulties arise in the calculation of the problem with conditions (2.1). As in the method of left trial run [8], let

$$\psi_{i+1}^j = \alpha_{i+1}^j \psi_i^j + \beta_{i+1}^j \tag{2.3}$$

($\psi_{i+1}{}^j = \psi((i + 1)h_1, jh_2)$, h_2 is the mesh with respect to θ; $\alpha_{i+1}{}^j$, $\beta_{i+1}{}^j$ are correction

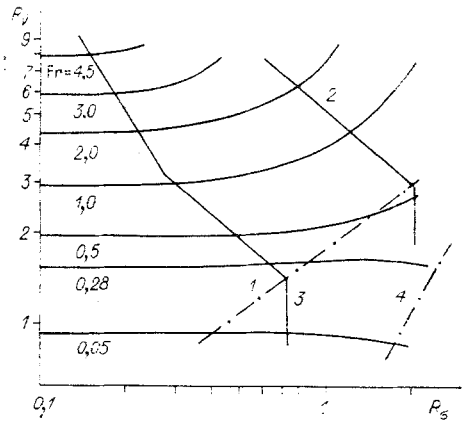

Fig. 2

factors). Then with i = 1 we have the following difference approximation of (2.1):

$$\psi_1^j = \psi_1^{m-j+1}, \quad A^j \frac{\psi_2^j - \psi_1^j}{h_1} + B^j \frac{\psi_1^j - \psi_1^{j-1}}{h_2} = A^{m-j+1} \frac{\psi_2^{m-j+1} - \psi_1^{m-j+1}}{h_1} + B^{m-j+1} \frac{\psi_1^{m-j+1} - \psi_1^{m-j}}{h_2}.$$

Adding the relations from (2.3) with i = 1

$$\psi_2^j = \alpha_2^j \psi_1^j + \beta_2^j, \quad \psi_2^{m-j+1} = \alpha_2^{m-j+1} \psi_1^{m-j+1} + \beta_2^{m-j+1},$$

we obtain four equations to determine $\psi_1{}^j$, $\psi_1{}^{m-j+1}$, $\psi_2{}^j$, $\psi_2{}^{m-j+1}$. Excluding $\psi_2{}^j$, $\psi_2{}^{m-j+1}$, we find

$$\psi_1^j = \frac{(B^j + B^{m-j+1})\,\psi_1^{j-1}/h_2 + (A^{m-j+1}\beta_2^{m-j+1} - A^j\beta_2^j)/h_1}{A^j(\alpha_2^j - 1)/h_1 - A^{m-j+1}(\alpha_2^{m-j+1} - 1)/h_1 + (B^j + B^{m-j+1})/h_2} \tag{2.4}$$

(m is the number of points along θ, $j \in [1, j^*]$, j^* is the number of points on Γ_1, Γ_2). It can be shown that the denominator in (2.4) does not vanish. We proceed in a similar manner to obtain the expression for $\omega_1{}^j$. All of the correction factors $\alpha_{i+1}{}^j$, $\beta_{i+1}{}^j$ (i = m − 2, ..., 1) are calculated beforehand for each value of j on the basis of formulas obtained by the left trial run method [8]. Thus, conditions (2.1) are realized exactly in each iteration.

3. Results of Calculations. The solution of the original problem obviously depends on four independent dimensionless parameters. As these parameters, we can take Re, We, $\lambda = a/R_k$, and L. Calculations were performed for $\lambda = 0.2$ and L = 20. A comparison with the data in [5] can be made for certain values of Re and We, when the wake of the bubbles is small.

The results of the calculations are shown in Fig. 2 by isolines of the Froude number $Fr = u^2/ga$ in the coordinates $R_\sigma = a/(\sigma/\rho g)^{1/2}$, $R_\nu = a/(\nu^2/g)^{1/3}$. Considering that $(R_\sigma/R_\nu)^6 = g\rho^3\nu^4/\sigma^3 = M$ (where M is the Morton number), we can easily find the upward velocity u for a bubble of the given size a in the specified fluid. Since we chose $\log R_\sigma$ and $\log R_\nu$ as the coordinates in Fig. 2, each fluid is represented by a certain straight line inclined 45° to the axis R_σ. It should be noted that upward velocity of the bubble increases with an increase in its size for fluids with a large value of M (which are generally fairly viscous fluids). In fluids with small M – shown by the straight line above line 1 – the dependence of the upward velocity of the bubble on its size is nonmonotonic in character. There is a local velocity maximum at a certain value of a. This corresponds to the case when isoline Fr = const is tangent to the straight line representing the fluid in Fig. 2. The value of Fr (upward velocity) decreases with a further increase in R_σ (the dimension a). The calculations showed that the point of the local velocity maximum corresponds to the moment of formation of a trailing vortex behind the bubble. A closed wake exists behind the bubble above the upper straight line 2 in Fig. 2. The left corner demarcated by line 3 is the region of spherical bubbles. Line 1 indicates that the leading portion of the bubble begins to advance, while line 4 indicates that the trailing portion begins to move backward. Thus, at Re < 0.4, the bubble begins to be distorted by the presence of the walls and stretches

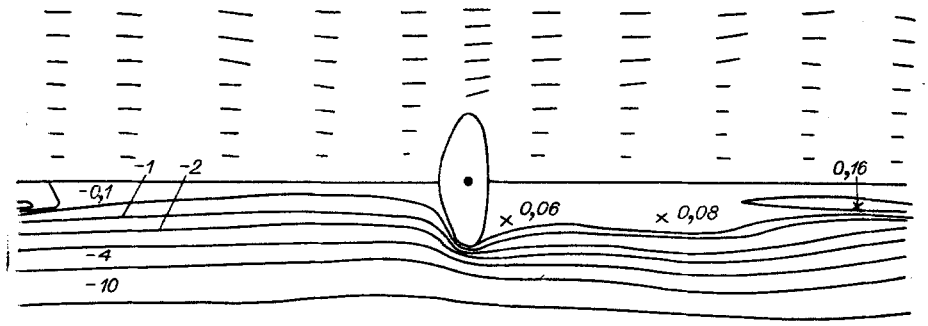

Fig. 3

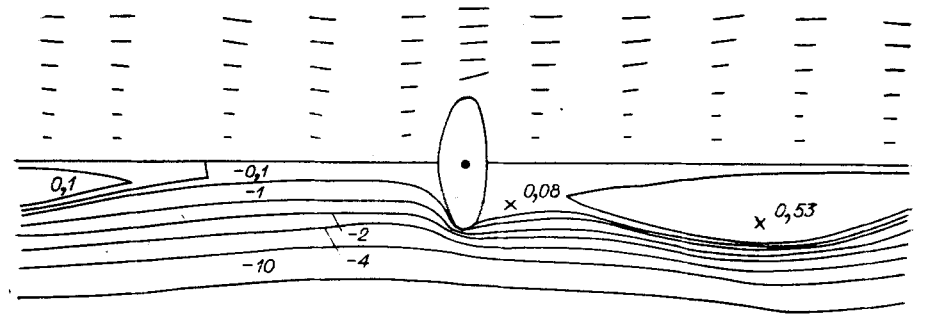

Fig. 4

out along the tube axis. In the region of spherical bubbles, the isolines Fr = const are nearly straight and correspond to a constant value of Re.

At Re < 20, the values of Fr and the flow pattern agree well with the calculations in [5]. Calculations performed with Re ≥ 20 yield values of Fr that differ 10-15% from the values in [5]. The lines indicating the presence of a trailing vortex and a region of spherical bubbles are located somewhat below the position dictated by the calculations in [5]. This can be attributed to the fact that we had twice as many points along θ as [5]. There are also significant differences in the form of the trailing vortex, the latter being considerably longer in our case. Figure 3 shows the flow pattern for Re = 40, We = 8.4, M = 0.00043, R_σ = 2.04, R_ν = 7.43. On the whole, the parameters and structure of the flow are similar to [9].

The good agreement between the calculations in [5] and experiments in [9] with regard to the drag coefficient (or, equivalently, with respect to Fr) is due to the fact that the main contributions to the integral characteristics are made by the separation zone (which was present in [5]) and the flow near the bubble. The drag coefficients begin to approach one another when the form of the free surface and the separation point are similar. The length of the wake is determined by the presence of a secondary flow. The presence of this flow is indicated in Fig. 3 by the local stream-function maximum of 0.16.

The above-constructed algorithm makes it possible to almost exactly determine the structure of the wake of the bubble. In truth, it is impossible to exactly satisfy the boundary conditions on the external boundary of the flow when solving the problem of the motion of a single bubble in an infinite region. It is usually necessary to take them at a certain finite distance. In addition, it is not entirely certain what conditions should be assigned behind the bubble. In the given formulation, everything depends on the distance between bubbles 2L. Given sufficiently large L, one bubble will have little effect on another. This effect can be evaluated experimentally.

Figure 4 shows the flow pattern for Re = 60, We = 9.6, M = 0.0001, R_σ = 1.9, R_ν = 8.8, Fr = 1.14. A separation zone and a developed secondary flow are present in the wake behind the bubble. The region of the intensive secondary flow, occupying nearly the entire space between bubbles, approaches the leading bubble with an increase in We.

Calculations performed with L = 10 showed that even at Re > 20 the wake from the leading bubble closes on the trailing bubble. Thus, instead of a chain of individual (surrounded

by fluid) bubbles rising toward the surface, we now have a more integrated structure consisting of bubbles and intervening fluid. The upward velocity of this chain is greater than the upward velocity of the individual bubbles and is determined by the buoyancy of the bubbles comprising the chain. The fluid entrained by the bubbles is displaced upward as such chains move toward the surface.

Calculations performed for another limiting case (surfacing of chains of bubbles in channels whose radius is comparable to a ($\lambda = 0.8$) showed that their upward velocity and the flow pattern are the same as in the surfacing of a single bubble if the distance between bubbles is greater than the diameter of the channel. This conclusion is fully in accord with the calculations in [3], where it was found that the velocity profile for the cross section of the tube smooths out at a distance of just 1.5 tube diameters from the bubble.

LITERATURE CITED

1. V. E. Nakorjakov, O. N. Kashinsky, and B. K. Kozmenko, "Experimental study of gas liquid slug flow in a small-diameter vertical pipe," Int. J. Multiphase Flow, 12, No. 3 (1986).
2. P. K. Volkov and B. G. Kuznetsov, "Numerical solution of a problem on the steady flow of a viscous liquid past a gas bubble in a tube," ChMMSS, 13, No. 5 (1982).
3. P. K. Volkov, "Surfacing of a gas bubble in a tube filled with a viscous liquid," Zh. Prikl. Mekh. Tekh. Fiz., No. 6 (1989).
4. V. P. Sirochenko, "Numerical solution of a problem concerning the flow of a viscous incompressible fluid in a doubly connected region," ChMMSS (Novosibirsk), 8, No. 1 (1977).
5. C. I. Christov and P. K. Volkov, "Numerical investigation of the steady viscous flow past a stationary deformable bubble," J. Fluid Mech., 158, 341 (1985).
6. A. Tom and K. Éiplt, Numerical Calculations of Fields in Engineering and Physics [in Russian], Énergiya, Moscow–Leningrad (1964).
7. E. L. Tarunin, "Optimization of implicit schemes for the Navier-Stokes equations in the variables of stream function and vorticity," Fifth All-Union Seminar on Numerical Methods of the Mechanics of Viscous Fluids. Computer Center, Siberian Department of the Soviet Academy of Sciences, Novosibirsk (1985), Vol. 1.
8. A. A. Samarskii and E. S. Nikolaev, Methods of Solving Network Equations [in Russian], Nauka, Moscow (1978).
9. D. Bhaga and M. E. Weber, "Bubbles in viscous liquids: shapes, wakes, and velocities," J. Fluid Mech., 105, 61 (1981).

STABILITY OF AN ADIABATIC CONTINUOUS CHEMICAL REACTOR

T. A. Bodnar'

UDC 532.72

Numerical studies (see [1-3], for example) have shown that there can be many steady-state regimes of operation of chemical reactors with distributed parameters. At the same time, as was demonstrated by N. N. Moiseev et al. in a postscript to [4], numerical methods cease to work for such systems in the neighborhood of bifurcation points – where the solution loses its uniqueness. Formidable obstacles are encountered in attempts to develop numerical methods of post-bifurcation analysis that make it possible to find all of the solutions emanating from bifurcation points. These obstacles are particularly great in the case of multidimensional problems or problems with many factors, such as in numerical studies of chemical reactors with distributed parameters.

In the present investigation, we use the theory in [4] to develop a method of analyzing the stability of steady-state solutions of a system of partial differential equations which describes the operation of a continuous chemical reactor with an adiabatic temperature change. The method is based on reduction of the number of dimensions of an infinite-dimensional problem through the use of projections of its solutions on an eigenfunction space and the Fredholm

Biisk. Translated from Zhurnal Prikladnoi Mekhaniki i Tekhnicheskoi Fiziki, No. 3, pp. 91-97, May-June, 1991. Original article submitted December 11, 1989.